Supplementary Information

Advancing the next generation nanolithography with infiltration synthesis of hybrid nanocomposite resists

Nikhil Tiwale,[a] Ashwanth Subramanian,[b] Kim Kisslinger,[a] Ming Lu,[a] Jiyoung Kim,[c] Aaron Stein,[a] and Chang-Yong Nam [a,b]*

[a]*Center for Functional Nanomaterials, Brookhaven National Laboratory, Upton, New York 11973, United States.*
**E-Mail: cynam@bnl.gov*
[b]*Department of Materials Science and Chemical Engineering, Stony Brook University, Stony Brook, New York 11794, United States.*
[c]*Department of Materials Science and Engineering, University of Texas at Dallas, Richardson, Texas 75080, United States.*

Table S1. E-beam dose (μC/cm^2) matrix depicting the dose array exposed for patterning exposure dose matrix

50	100	150	200	250
300	350	400	450	500
600	700	800	900	1000
1100	1200	1300	1400	1500
1750	2000	2250	2500	2750
3000	4000	5000	6000	7000

Table S2. Summary of ICP-RIE conditions used in the study

Process	Temp. (°C)	Pressure (mTorr)	RF Power (W)	ICP Power (W)	Gas flow rate (sccm)
O_2 Etch	20	30	200	0	O_2: 50
SiO_2 Etch	25	15	40	700	O_2: 1.5 CHF_3: 50
Cryogenic Si Etch (etch rate)	-100	15	15	800	O_2: 12 SF_6: 40
Cryogenic Si Etch (nanopatterns)	-100	15	15	800	O_2: 16 SF_6: 40

Supporting Figures

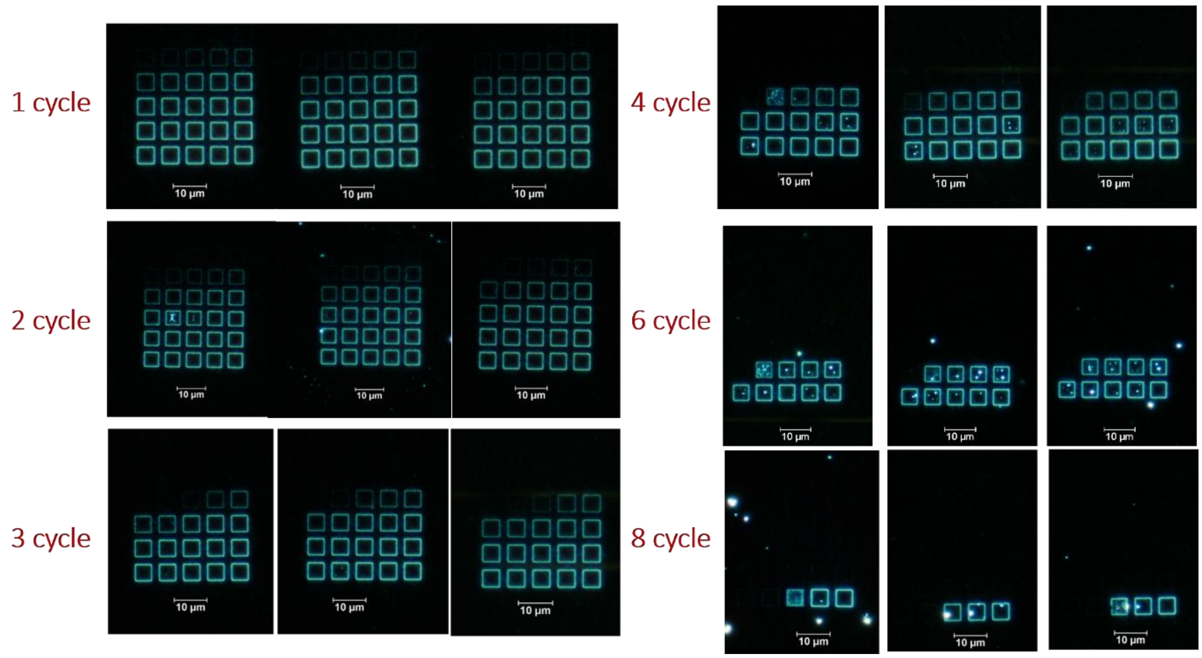

Figure S1. Dark-field optical microscopy images of as developed exposure dose test array of samples subjected to different infiltration cycles showing consistency of dose-to-clear across samples.

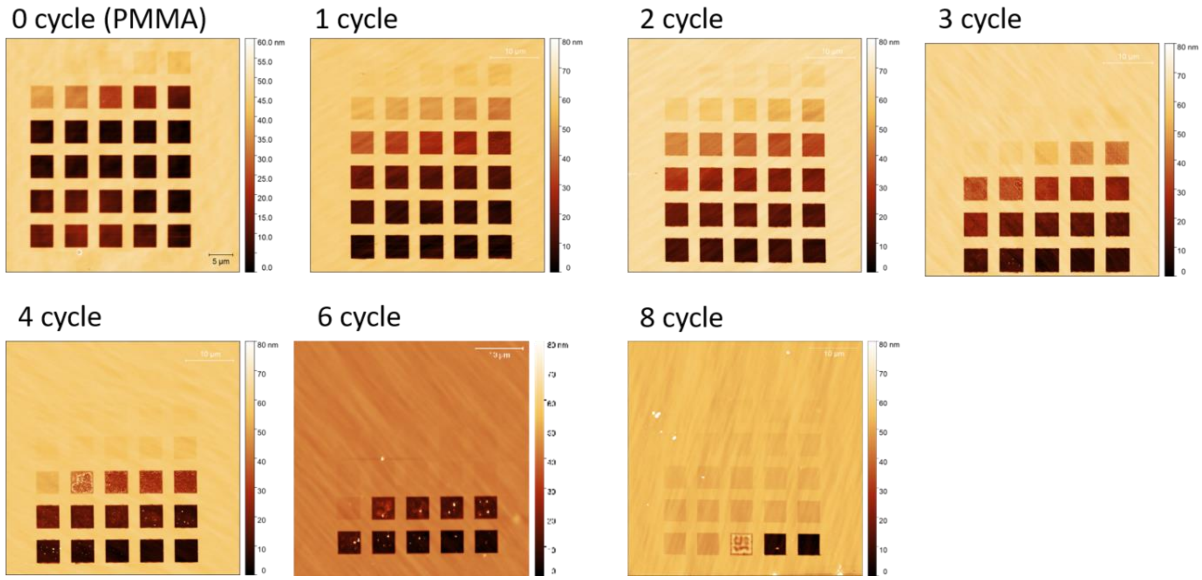

Figure S2. AFM height maps of exposure dose matrix patterned as per the dose array illustrated in Table S1. With increasing infiltration cycles, the dose-to-clear can be seen to increase.

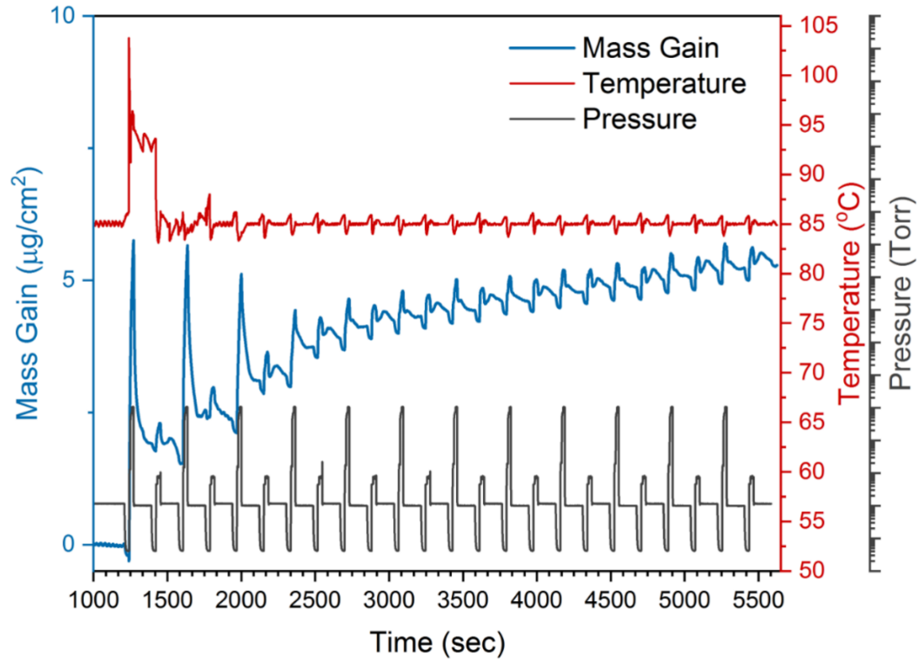

Figure S3. As acquired QCM measurement showing temporal change in mass gain per area, ALD chamber temperature, and pressure against the measurement time for 12 infiltration cycles. In the pressure variation plot, the larger pulse corresponds to TMA half cycle, whereas the smaller pulse depicts water half cycle and the dip in pressure signifies chamber purge step.

Section S1. Estimation of elemental composition of infiltrated hybrid resists

The mass gain data (Fig. S3) measured by in-situ QCM experiments can be used to estimate the elemental composition of AlO_x-infiltrated PMMA by assuming that the infiltrated precursors form stoichiometric Al_2O_3, which is homogeneously distributed within the PMMA matrix. Specifically, we can convert the mass gain per area value to the number of Al and O atoms added for the given number of infiltration cycles by using following expressions:

$$[no. of\ Al\ atoms\ gained/area] = \frac{[wt. gain/area]\ \times\ 2 \times\ N_A}{(2\ X\ [Atomic\ wt. of\ Al] +\ 3\ \times\ [Atomic\ wt. of\ O])}$$

$$[no. of\ O\ atoms\ gained/area] = \frac{[wt. gain/area]\ \times\ 3}{(2\ X\ [Atomic\ wt. of\ Al] +\ 3\ \times\ [Atomic\ wt. of\ O])}$$

, where N_A is Avogadro number, atomic wt. of Al is 26.98 g/mol and atomic wt. of O is 15.99 g/mol. Furthermore, the wt. % of Al gained for the given number of infiltration cycles can be estimated as:

$$[Al\ wt. gain/area] =\ [no. of\ Al\ atoms\ gained/area]\ \times\ [Atomic\ wt. of\ Al]$$

Meanwhile, using the PMMA density ~ 1.18 g/cm^3 and the film thickness ~60 nm, the wt. of the PMMA thin film can be estimated as,

$$[PMMA\ thin\ film\ wt./area] = [Density\ of\ PMMA]\ \times\ [Thickness\ of\ PMMA\ thin\ film]$$

, which calculates to 7.08 µg/cm^2. Additionally, assuming that the atomic composition in PMMA is the same as that in its monomer methyl methacrylate(MMA or $C_5H_8O_2$), the no. of C and O atoms per area can be estimated as,

$$[no. of\ C\ atoms\ in\ PMMA\ film/area] = \frac{[PMMA\ thin\ film\ wt./area]\ \times\ 5}{[Molecular\ wt. of\ MMA]} =$$

$$[no. of\ O\ atoms\ in\ PMMA\ film/area] = \frac{[PMMA\ thin\ film\ wt./area]\ \times\ 2}{[Molecular\ wt. of\ MMA]}$$

, where molecular wt. of MMA is 100.121 g/mol. The total no. of O atoms for the given number of infiltration cycles would then be the sum of no. of O atoms in PMMA and no. of O atoms gained by infiltration of AlO_x (Al_2O_3). Based on these estimations the evolution of no. of atoms of Al and O as well as atomic ratio of Al to C are illustrated in Fig. S4.

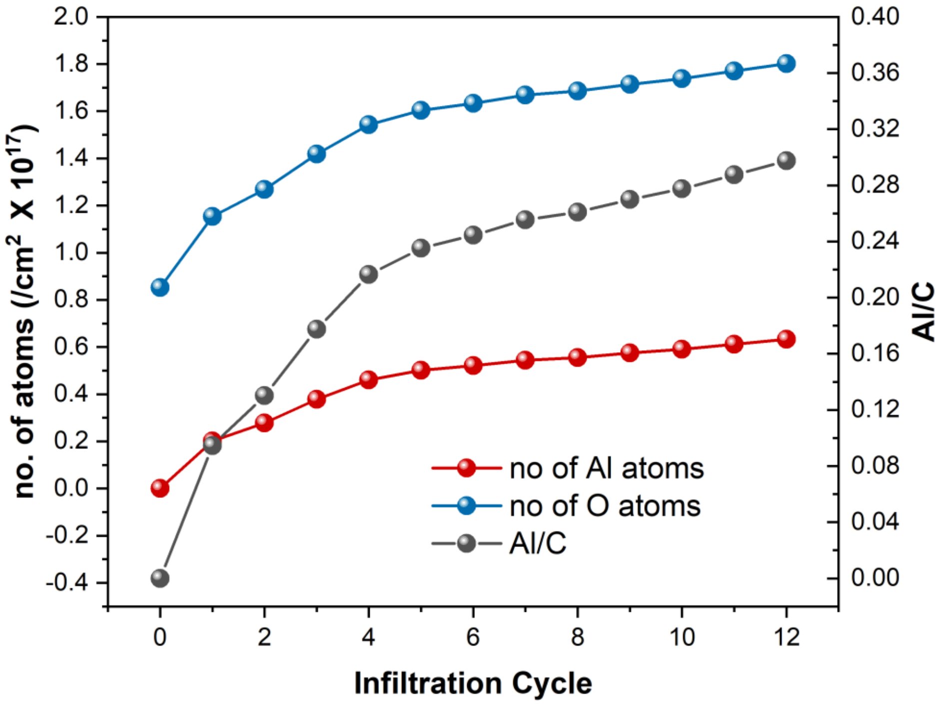

Figure S 4 Evolution of estimated no. of Al and O atoms with increasing number of infiltration cycles (left axis) and atomic ratio or Al to C within the synthesized hybrid resist (right axis).